Journal of Molecular Modeling (2022) 28: 202
https://doi.org/10.1007/s00894-022-05184-x

ORIGINAL PAPER

Peptide mediated colorimetric detection of SARS-CoV-2 using gold nanoparticles: a molecular dynamics simulation study

Nitu Verma[1] · Yogesh Badhe[1] · Rakesh Gupta[1] · Auhin Kumar Maparu[1] · Beena Rai[1]

Received: 27 December 2021 / Accepted: 7 June 2022 / Published online: 24 June 2022

Abstract

The outbreak of severe acute respiratory syndrome coronavirus 2 (SARS-CoV-2) has necessitated the development of a rapid, simple yet selective naked-eye detection methodology that does not require any advanced instrumental techniques. In this study, we report our computational findings on the detection of SARS-CoV-2 using peptide- functionalized gold nanoparticles (GNPs). The peptide has been screened from angiotensin-converting enzyme 2 (ACE2) receptor situated on the surface of the host cell membrane which interacts with the spike protein of SARS-CoV-2, resulting entry of the virus into the host cell. As a result, the peptide-functionalized GNPs possess excellent affinity towards the spikes of SARS-CoV-2 and readily get aggregated once exposed to SARS-CoV-2 antigen or virus. The stability of the peptides on the surface of GNPs and their interaction with the spike protein of the virus have been investigated using coarse-grained molecular dynamic simulations. The potential of mean force calculation of spike protein confirmed strong binding between peptide and receptor-binding domain (RBD) of spike protein. Our in silico results demonstrate the potential of the peptide-functionalized GNPs in the development of simple and rapid colorimetric biosensors for clinical diagnosis.

Keywords Covid-19 detection · SARS-CoV-2 · Gold nanoparticle · Colorimetric detection · Peptides · Molecular dynamics simulation

Introduction

For the past 2 years, COVID-19 pandemic has posed a serious threat against public health and global economies [1–3]. Along with the suitable therapeutics to cure this deadly disease, rapid diagnosis and isolation of infected persons are being adopted to contain the spread of the virus worldwide [4–6]. At present, nucleic acid testing is the primary method for diagnosing COVID-19 [5]. RT-PCR (reverse transcription polymerase chain reaction) kits have been designed to detect SARS-CoV-2 genetically by reverse transcription and amplification of its RNA into complementary DNA [7, 8]. Serological tests based on the presence of viral antibodies in the blood of exposed individuals are also being developed to understand the full extent of viral spread [9]. CT scans have been used for clinical diagnosis of COVID-19 in some areas [10]. Other emerging diagnostic tests based on nucleic acid testing (LAMP [11], SHERLOCK [12]) and protein testing (ELISA [13]) have also been reported. All these biosensing techniques mostly require advanced instruments and need of an expert, which are time-consuming and cumbersome as well as susceptible to viral gene mutation [7, 14].

Efforts have been made for the development of simple, reliable, and rapid detection methodologies [14–16]. In this regard, gold nanoparticles (GNPs) have been extensively utilized for developing colorimetric detection platform owing to their exceptional optical properties such as high extinction coefficient, localized surface plasmon resonance, and inherent photostability [14, 16]. For example, Moitra et al. used GNPs capped with suitably designed thiol-modified antisense oligonucleotides (ASOs) specific for nucleocapsid phosphoprotein (ssDNA) of SARS-CoV-2 RNA for selective "Naked-eye" detection of SARS-CoV-2 [14]. The thiol-modified ASO-capped GNPs agglomerate selectively in the presence of its target RNA sequence of SARS-CoV-2

✉ Rakesh Gupta
gupta.rakesh2@tcs.com

✉ Auhin Kumar Maparu
auhin.maparu@tcs.com

[1] Physical Sciences Research Area, Tata Research Development and Design Centre, TCS Research, Tata Consultancy Services, 54B, Hadapsar Industrial Estate, Pune 411013, India

and demonstrate a change in its surface plasmon resonance (SPR) and subsequent color change of the solution (Fig. 1a). The technique, however, required extensive process of viral RNA extraction, isolation, and replication. The other important technique was proposed by Seo et al., where they used graphene surface for preferential binding of S-protein to its antibody [15]. FET-based sensor was attached to the graphene surface for the detection of the virus. The technique also requires complex system setup as shown in (Fig. 1b). Functionalized GNPs and their interaction with viral surface structural protein have been proposed previously for other viruses as well [17, 18]. Niikura et al. used GNPs coated with sialic acid–linked lipids for the optical detection of JC virus-like particles [17]. Zheng et al. proposed detection of influenza viruses with glycan-functionalized GNPs [18].

It has been well established that the spike proteins of SARS-CoV-2 are responsible for the virus invasion and disease spread [19–22]. Accordingly, anti-spike antibodies have been developed and attached on the surface of gold nanoparticles to induce aggregation in presence of SARS-CoV-2 or the antigen itself [23–25]. However, antibodies are associated with their inherent limitations such as large molecular size, cross-reactivity, high production, and poor stability [5, 7]. Rationally designed peptides with high specificity to the target antigen can be a potential alternative to these antibodies. Accordingly, in our recent work, we have screened potential peptides for targeting spike proteins of SARS-CoV-2 based on their stability in aqueous solution and binding affinity to spike protein [26]. Since the RBD of spike proteins of SARS-CoV-2 interact preferentially with ACE2 receptors [20, 21], the peptides were derived from ACE2. In the present work, we have utilized one of these potential peptides for functionalizing GNPs. The peptides not only impart strong affinity towards SARS-CoV-2 spikes to the GNPs, but also provide excellent stability to the GNPs in aqueous environment, as demonstrated by molecular dynamics simulation. Furthermore, our in silico study shows aggregation of GNPs in presence of SARS-CoV-2 antigen or virus which will be associated with visual change in color of the GNP dispersion (Fig. 1c).

Overall, the current study demonstrates a potential design paradigm for colorimetric detection of SARS-CoV-2 or its antigen using peptide modified GNPs.

Materials and methods

The peptide structure (amino acid sequence- EQEERIQQDKRKNENEDKRYQRYGRGKGHQP) was taken from Badhe et al. [26]. Badhe et al. reported several peptides which could selectively bind to the receptor-binding domain (RBD) of the spike protein of the coronavirus. They have screened several peptides based on their stability in aqueous solution and binding free energies. The peptide (EQEERIQQDKRKNENEDKRYQRYGRGKGHQP) was found to be more stable and had lowest binding energy. The structure of full-length SARS-COV-2 spike protein model in a viral membrane was taken from the work of Woo et al [27, 28] and structure of spike RBD was taken from PDB ID 6M0J [21]. The peptide and spike protein were modelled using the MARTINI force field [29]. The peptides, proteins, and lipids were converted to CG models using the script available at MARTINI force field developer's website [30, 31].The coarse-grained (CG) parameters of thiol-coated GNPs were taken from previous simulation studies [32–34]. The gold nanoparticle was carved out from an FCC crystal of given size of nanoparticle. A one-to-one mapping of atomistic atom to CG atom was used. Four atomistic SPC water molecules were taken together to represent a single CG MARTINI bead for water. The peptide was bound to the GNPs through a thiol bond giving the GNP-peptide complex (Au-S- EQEERIQQDKRKNENEDKRYQRYGRGKGHQP). The GNP functionalization was done based on stability of GNP-peptide complex reported in literature [35]. All simulations were performed using GROMACS 2018 software [36–38] and visualized using VMD 1.9.1 [39].

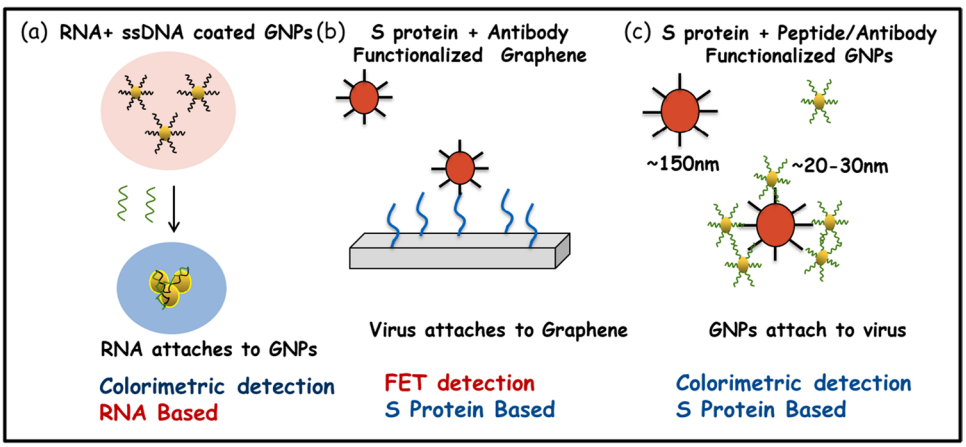

Fig. 1 Schematics for detection techniques for SARS-CoV-2. **a** RNA-based colorimetric detection using GNPs [14]. **b** FET-based biosensing using preferential binding of S protein to antibody functionalized Graphene [15]. **c** S protein–based colorimetric detection using antibody [16]/peptide (present study) functionalized GNPs

The peptide-coated GNP was simulated in the aqueous solution for proper functionalization of the GNPs. Furthermore, agglomeration of peptide-coated GNPs is studied to analyze the stability of the system. Finally, binding of spike protein with peptide-coated GNPs is observed. The schematic diagram of the present study is shown in Fig. 2.

The peptide-coated GNPs and spike were energy minimized individually in vacuum. The structures were solvated with water and ions were added to neutralize the system. Again, the systems were energy minimized and further simulated under NVT (10 ns) and NPT (10 ns) ensemble. During these equilibration runs, the peptide-coated GNPs and spike were restrained at their position. These systems were further simulated without restraints for 0.5 μs at $T = 300$ K and 1 bar pressure. The pressure was coupled isotopically with the compressibility of 4.5×10^{-5} bar^{-1}. Temperature and pressure were controlled by v-rescale thermostat and Parrinello-Rahman barostat with a time constant of 2 ps and 12 ps, respectively. The reaction field method was used for the treatment of the long-range electrostatic interactions. All bonds of the proteins and peptides were constrained using LINCS algorithm.

The umbrella sampling simulations were performed to compute the binding affinity of GNPs with the spike. The initial configurations were generated using system simulated for 1.5 μs. The spike protein was slowly pulled from the GNP at a constant speed of 0.01 nm/ps. Whenever the distance between the center of the mass of RBD and peptide changed by 0.2 nm, that configuration was kept for further simulations. The force constant of 1000 kJ mol^{-1} nm^{-2} was used to keep the spike restrained at its respective position. Each extracted configuration was simulated for 0.2 μs and was used for the potential of mean force calculation. The potential of mean force was generated using the weighted histogram analysis method (WHAM) [40].

Results and discussion

Stability of peptide-coated GNPs

Functionalization of GNPs with peptides

Three different-sized nanoparticles (3, 6, and 10 nm) were used in this study. At first, we performed functionalization of GNPs with the peptide. Six peptides were attached to the GNP of diameter 6 nm through a thiol bond. Thiols are generally used for functionalizing GNPs due to the excellent affinity of gold towards thiol groups [41]. The system was solvated, neutralized, minimized, and subsequently equilibrated. The equilibrated structure of peptide-coated GNPs in aqueous solution was analyzed. We found that after 0.3-μs equilibration, the peptides cover-up the GNP nicely as shown in Fig. 3a. Similar functionalization of GNP was also done with 12 peptides as shown in Fig. 3b. We conclude that the peptides spread across the NP surface nicely resulting in not only good functionalization of the NP but also aid in stabilization of the nanoparticles. Similar results were obtained for 3- and 10-nm GNP systems and results of the same are shown in Figs. S1 and S2 respectively (please see supporting information section S1).

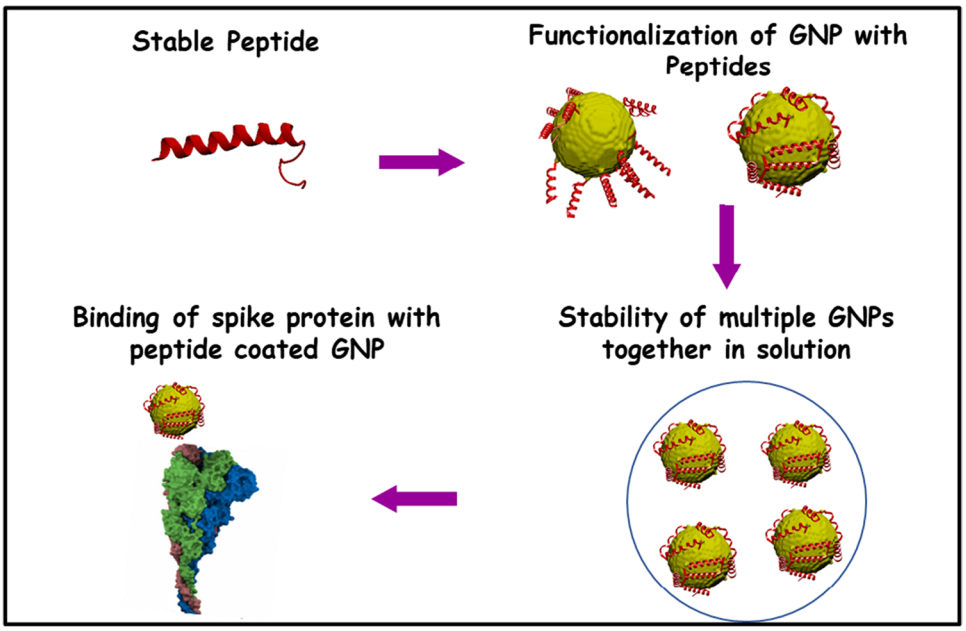

Fig. 2 Schematic representation of detection of spike protein using peptide-coated GNP. The images are rendered using VMD software

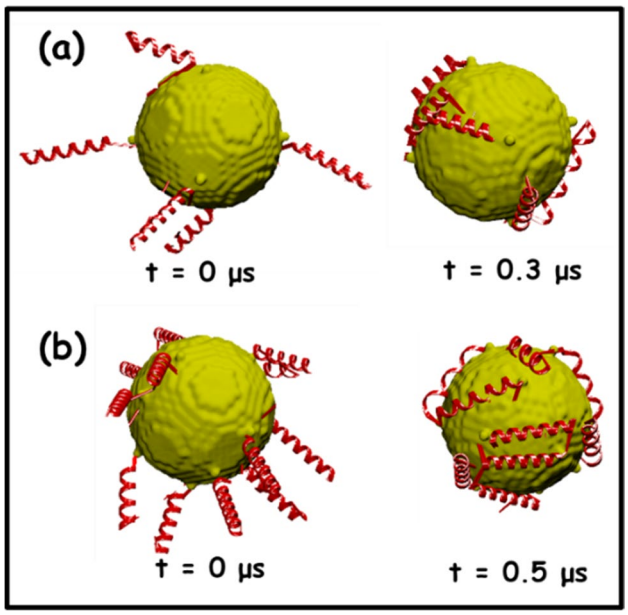

Fig. 3 Peptide functionalization study of GNPs of diameter 6 nm coated with **a** 6 peptides and **b** 12 peptides. Peptides spread across the NP surface nicely resulting in good functionalization. *(Color scheme: yellow—GNP, red—peptide) (All simulations are done in aqueous solution. Water beads are not shown for clarity)*

Aggregation of peptide-coated GNPs in aqueous solution

Nanoparticles (NPs), owing to their small size, have very high surface energy and tend to agglomerate in solution. We quantify aggregation based on agglomeration of GNPs at a close enough distance that would lead to colorimetric detection. The surface plasmon resonance shift needed for this strongly depends on the interparticle distance, particle size, and the number of coupled particles [17]. As aggregation leads to change in plasmon response, for our study, we want the GNPs to aggregate due to binding with the spike and not on their own. So, the GNPs need to be stable (no aggregation in the absence of spike protein) in the solution. Peptide in our study has negative charge and peptide-coated GNPs repel each other due to this charge. Therefore, functionalization of GNPs with peptide can improve the stability of GNPs in aqueous environment. However, the stability will depend on whether the repulsive forces among the adjacent GNPs are strong enough to overcome the attractive forces arising from high surface energy.

The GNPs tend to aggregate in absence of any peptide modification (supporting information Fig. S3). When 6 peptides were coated on 6-nm GNPs, the GNPs in solution still tend to agglomerate (Fig. 4a). This was further confirmed

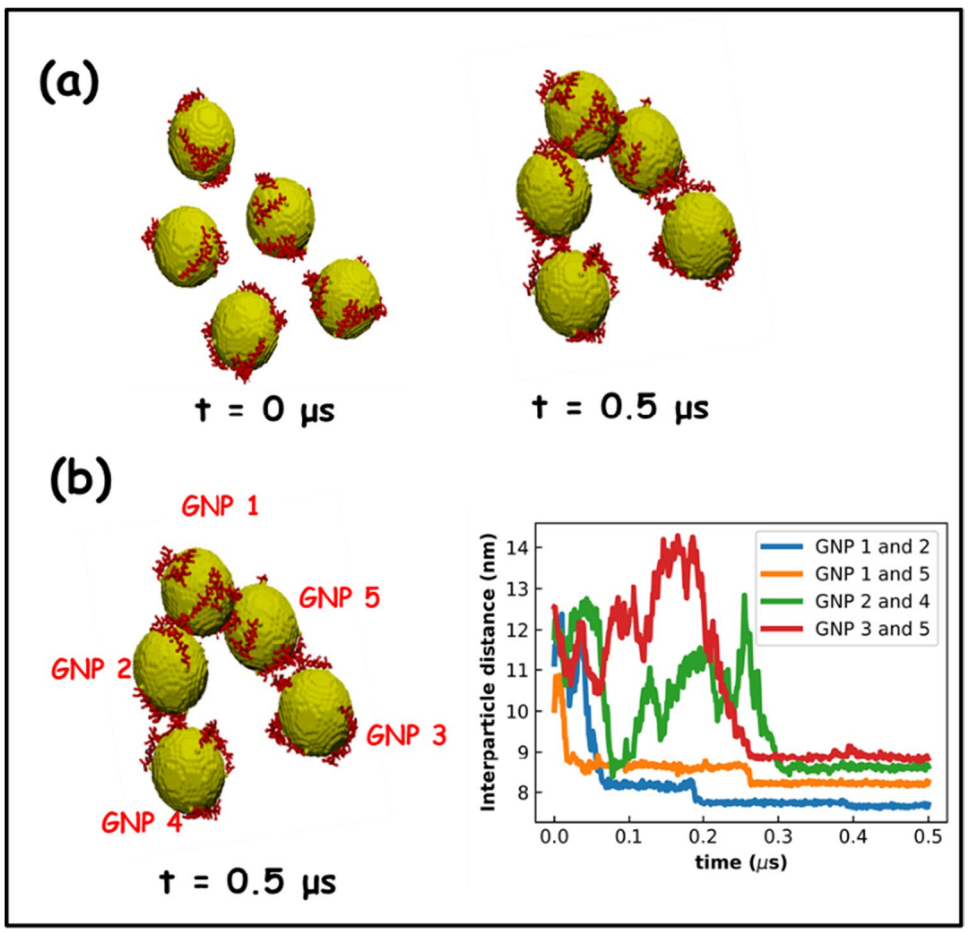

Fig. 4 **a** Aggregation study of GNPs of diameter 6 nm coated with 6 peptides **b** interparticle distance variation of the agglomerated GNPs. GNPs coated with 6 peptides agglomerate in solution. *(Color scheme: yellow—GNP, red—peptide) (All simulations were performed in aqueous solution. Water beads are not shown for clarity)*

by examining the interparticle distance variable of the GNPs (Fig. 4b). As the peptide-coated GNPs agglomerate, they form a cluster, and the interparticle distance between the GNPs that get attached to each other stabilizes.

Furthermore, we increase the coating on individual GNP to 12 peptides and simulate the system as shown in Fig. 5. The 6-nm GNPs coated with 12 peptides are found to be stable in aqueous solution. We can observe from Fig. 5a that the interparticle distance between all the GNPs in solution is always varying and does not stabilize; thus, the GNPs do not get attached to each other to agglomerate. This is further studied by simulating two 12 peptide-coated GNP in solution (Fig. 5b), which shows that there is repulsion between two GNPs leading to no agglomeration.

Similar study was performed for GNPs of diameter 3 nm, where it was found that the system is stable in aqueous solution when the GNP is coated with 4 peptides (see supporting information Fig. S4). For GNP of diameter 10 nm, at least 46 peptides are required to be coated on GNP for the system to be stable in aqueous solution (supporting information Fig. S5).

From stability analysis of peptide-coated GNPs of different sizes, we conclude that minimum peptide density required for the formation of stable GNP solution lies in the range of 0.11–0.15 peptides nm^{-2} as summarized in Table 1. Peptide density obtained here can be adopted as basis for coating this peptide on GNPs of higher sizes (~20–30 nm) for experimental study.

In this section, we have discussed that GNPs can easily be functionalized with peptides and stability of these coated nanoparticles depend upon the particle size and the density of the coated peptides. In the next section, we will discuss about the interaction of the spike protein of SARS-CoV-2 with peptide-coated GNPs.

Table 1 Minimum peptide density required to stabilize GNP solution for different sizes of GNPs

GNP diameter (nm)	Minimum no. of peptide required to stabilize GNP solution	Peptide density (no. of peptide per nm^2 of GNP surface)
3	4	0.14
6	12	0.11
10	46	0.15

Interaction of spike protein

Interaction between RBD spike protein and peptide-coated GNP

In the previous section, we investigated the stability of peptide-coated GNPs in solution. In this section, we have investigated the binding interaction between peptide-coated GNP and RBD protein (RBD taken from PDB ID:6M0J [21]). For this, the RBD protein was placed around 2 nm away from the peptide-coated GNP (size 6 nm, no. of peptides on a GNP = 12) and the system was simulated for 1.5 μs as shown in Fig. 6a. From the analysis of the trajectory, we found that RBD interacted with the peptide directly and strongly bound to it.

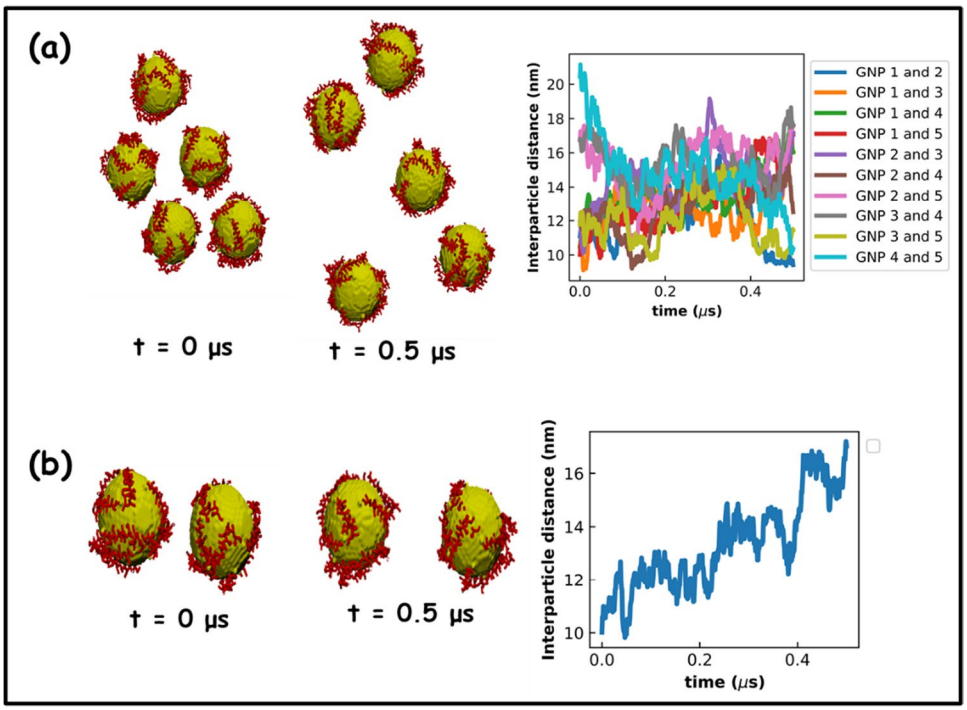

Fig. 5 Aggregation study of GNPs of diameter 6 nm coated with 12 peptides. **a** 5 peptide-coated GNPs do not agglomerate as confirmed from their interparticle distance that keeps on changing. **b** 2 peptide-coated GNPs repel each other showing increase in their inter-particle distance. Twelve peptide-coated GNPs do not agglomerate. *(Color scheme: yellow–GNP, red—peptide) (All simulations were performed in aqueous solution. Water beads are not shown for clarity)*

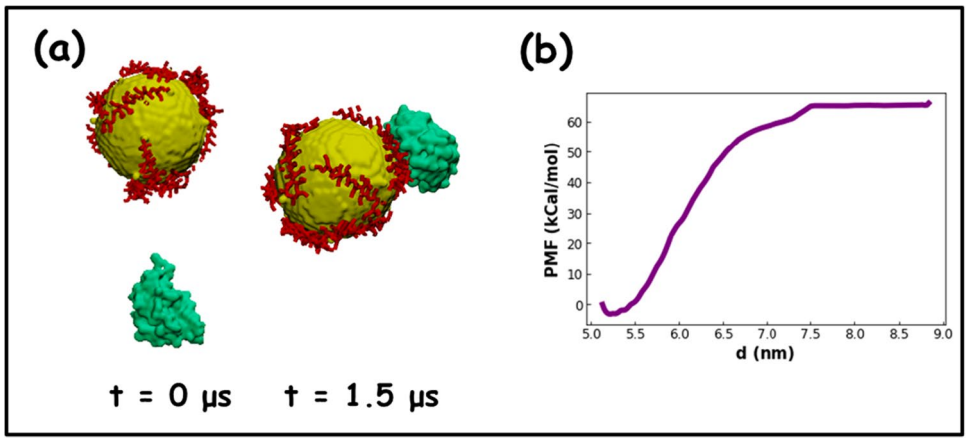

Fig. 6 **a** Initial and final configuration of the system simulated for 1.5 μs. Spike protein was kept 2 nm away from the peptide coated GNP (D ~ 6 nm, no of peptides 12) at t=0. **b** Potential of mean force (PMF) or free energy of RBD in complex with peptide-coated GNP. PMF gives the free energy for unbinding of spike and d is the distance between COM of peptide-coated GNP and spike protein. *(Color scheme: yellow—GNP, red—peptide, green—spike RBD protein, grey—lipids) (All simulations are done in aqueous solution. Water beads are not shown for clarity)*

To confirm above findings, we have also performed umbrella sampling simulations to obtain the free energy of the binding interaction between RBD and peptide. The details of the simulations can be found in the "Materials and methods" section. The free energy profile is shown in Fig. 6b. The binding free energy of RBD-peptide coated GNP complex was found to be −66 kCal mol^{-1}. This indicates strong binding between RBD protein and peptide [42, 43]. Similar study was performed for different configurations of RBD, and peptide-coated GNP, all resulted in RBD binding to peptide instead of directly interacting with GNP. From this, we conclude that the RBD prefers to bind strongly to the peptide coated on GNP. More details on umbrella sampling and free energy calculations can be found in the supporting information section S4. Please note, here, we have used GNP of 6 nm for computational ease; however, as shown in Table 1, bigger nanoparticle can easily be used as well with minimum surface peptide density.

Interaction between peptide-coated GNP and spike protein in bilayer

In the previous section, we have used the RBD of spike protein to study the interaction between spike protein and peptide-coated GNP which gives a good overview of how peptide binds to spike protein. As per Fig. 1, the peptide-functionalized GNPs must bind on the virus envelope. To mimic the real case scenario, simulation with full spike protein would be more meaningful. Hence, in this section, we have studied the interaction of peptide-coated GNPs with full-length homo-trimeric spike protein in viral membrane (bilayer). The atomistic structure of full spike protein in viral membrane was taken from Woo et al [27]. This structure was further coarse-grained using scripts on Martini website [30, 31, 44]. The RBD of spike protein in this structure is between residues 318 and 541 [27]. For binding analysis, the peptide-coated GNP was kept ~2 nm (surface to surface distance) away from the spike protein and the system was simulated in aqueous environment as shown in Fig. 7.

From Fig. 7, we observe that the spike protein binds to the peptides coated on the GNP. Proline residue of the peptide from GNP side makes first contact with phenylalanine (residue 456) of spike protein. This residue belongs to the RBD domain of the spike protein; subsequently, nearby residues of RBD bind to the GNP [27]. This conforms to the literature findings reporting RBD interaction

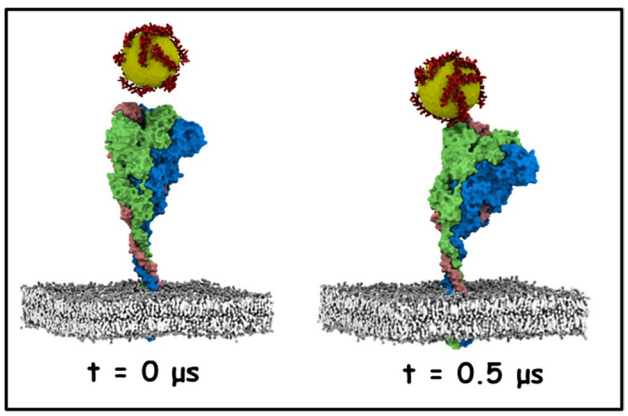

Fig. 7 Initial and final configuration of the system simulated for 0.5 μs. Peptide-coated GNP (D ~ 6 nm, no. of peptides=12) was kept ~2 nm away from spike protein in bilayer. *(Color scheme: yellow—GNP, red—peptide, blue/green/pink—three chains of spike protein, grey—lipids) (All simulations are done in aqueous solution. Water beads are not shown for clarity)*

with ACE2 receptor [20, 21] as the peptide used here is derived from ACE2 protein [26]. This further supports our proposal to use peptide-coated GNPs in biosensors for COVID-19 detection.

Further interaction between multiple peptide-coated GNPs and spikes in bilayer was investigated. First, we simulated 4 peptide-coated GNPs kept at a distance from 4 spike in bilayer as shown in Fig. 8a. The individual spike proteins were kept at distance of ~25 nm from each other as found on the viral membrane [45]. We observe that all 4 spike protein binds to individual peptide-coated GNPs kept closest to them. Increasing the number of peptide-coated GNPs to 6 while keeping no. of spike protein 4, we observe that three out of six GNPs directly bind to the spike (Fig. 8b). From these, we conclude that agglomeration of peptide-coated GNPs by binding to multiple spike protein is feasible, but we need to consider the repulsion between the functionalized GNPs as well as the attraction between these GNPs and spike protein.

The above study shows aggregation of GNPs in presence of multiple spike protein which will be associated with visual change in color of the GNP dispersion. Further study would require in vitro experimentation of entire virus or virus-like particles (VLPs) in the peptide-coated GNP solution, to demonstrate the colorimetric effect. The mechanism of colorimetric detection is significantly different here as compared to the simple dispersion or agglomeration of GNPs in solutions. Here, the GNPs are binding to the spike protein of the viral envelope due to interaction between the peptide and spike protein resulting in change in the separation distance between the NPs and that could give colorimetric detection [17, 18]. Our in silico study advocates for the effectiveness of the rationally designed peptide-coated GNPs for detection of SARS-CoV-2 and its antigen. Although antibody-mediated detection has been demonstrated recently [16] by Ventura et al. at in vitro level, the current study would still need in vitro validation using actual virus. It may be noted that the above-reported study required identification

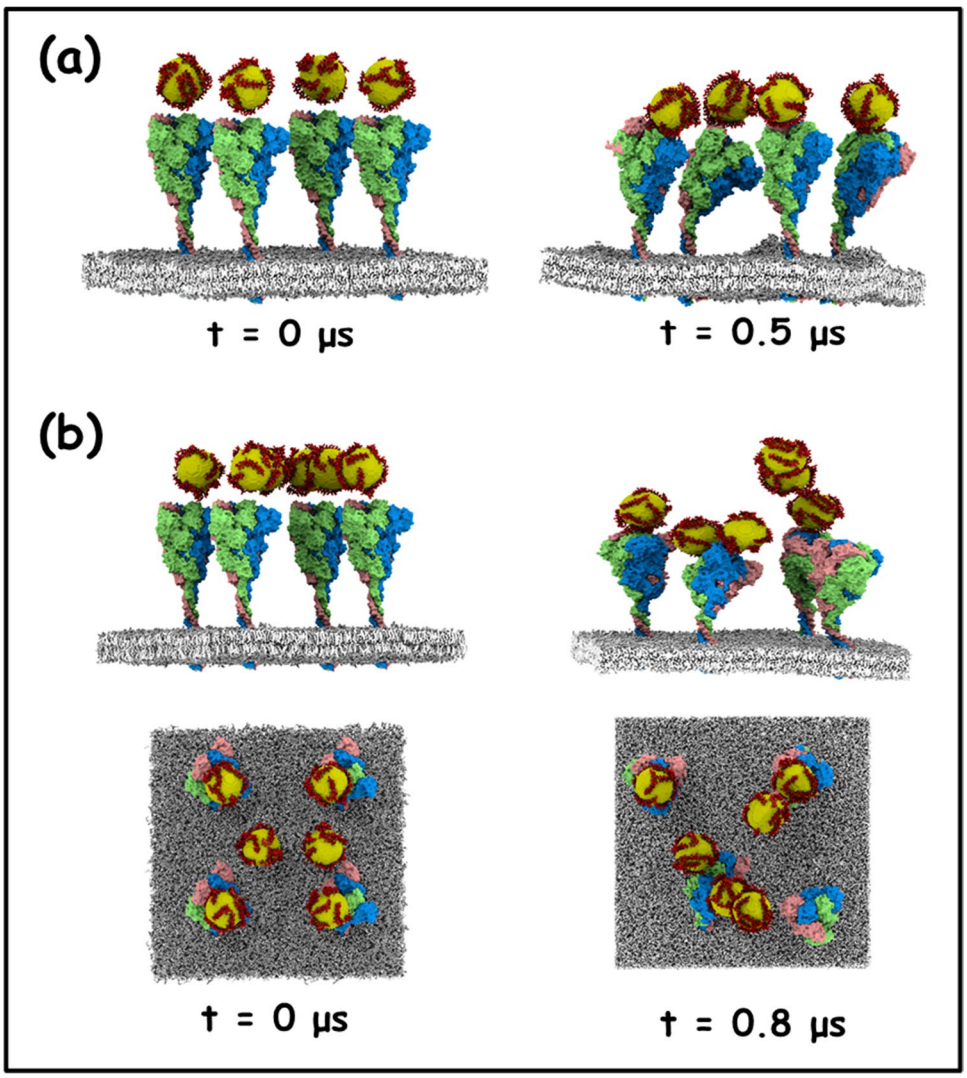

Fig. 8 Initial and final configuration of the **a** 4 peptide-coated GNPs (D ~ 6 nm, no. of peptides on each GNP=12) and 4 spikes in bilayer. All 4 of the GNPs bind to the spike. **b** Six peptide-coated GNPs and 4 spikes in bilayer. Three out of 6 peptide-coated GNPs in the case bind to spike. GNPs kept at 2 nm away vertically from the spikes. *(Color scheme: yellow—GNP, red—peptide, blue/green/pink—three chains of spike protein, grey—lipids) (All simulations are done in aqueous solution. Water beads are not shown for clarity)*

and preparation of antibodies for specific targeting of viral proteins and owing to larger size of antibodies, the steric hindrance on functionalized GNPs could limit the viral detection. In comparison, the peptide used in our study is much easier to prepare and is also much smaller. Our peptide has played the dual role of functionalizing the GNPs and targeting spike protein of SARS-CoV-2 without UV activation as required by antibody for detection of the virus. Also, in the above-mentioned study [16], excess of antibody is required to ensure full surface coverage whereas our study provides a guidance to use the peptides judicially based on their surface coverage and the size of GNPs. Thus, our proposed strategy can lead to much simpler and scalable production of virus-targeted GNPs and will surely guide future researchers to come up with more suitable colorimetric detection techniques using peptides and GNPs.

Conclusion

In this study, we have utilized the preferential binding of the spike protein of SARS-CoV-2 to the peptide screened from ACE2 receptor of the host cells and proposed a simple method for colorimetric detection of the virus based on plasmonic nature of GNPs. In particular, we have functionalized the GNPs with our screened peptide and analyzed their structural stability through molecular dynamics simulations. We have also determined the minimum peptide density required for GNPs of different sizes to prevent agglomeration. After stabilizing peptide-coated GNPs in aqueous solution, we have studied the interaction of spike protein with peptide-coated GNPs and found that the spike protein interacts preferentially with the peptides as proposed and, thus, can be utilized in biosensors. In future, the proposed detection strategy will be validated via in vitro experimentation using peptide-functionalized GNPs and actual SARS-CoV-2 antigen/virus.

Supplementary Information The online version contains supplementary material available at https://doi.org/10.1007/s00894-022-05184-x.

Acknowledgements The authors would like to thank Mr. K Ananth Krishnan, Corporate Technology Officer, Tata Consultancy Services, and Dr Gautam Shroff, Head of Research, Tata Consultancy Services, for their constant encouragement and support during this project.

Author contribution Nitu Verma, Rakesh Gupta, Auhin Maparu, and Beena Rai conceptualized the idea. Nitu Verma, Yogesh Badhe, and Rakesh Gupta have performed simulations. Nitu Verma and Yogesh Badhe have analyzed the results. All the authors contributed to discussing the results and writing and editing the manuscript.

Funding This research was funded by Tata Consultancy Services (TCS), CTO organization (grant number: 1009292).

Data availability The structure and topology files of bilayer and spike proteins are given in the supporting documents.

Code availability Not applicable.

Declarations

Competing interests The authors declare no competing interests.

References

1. WHO Coronavirus Disease (COVID-19) Dashboard. https://covid19.who.int/. Accessed 18 Oct 2021
2. Cucinotta D, Vanelli M (2020) WHO declares COVID-19 a pandemic. Acta Biomedica 91:157–160
3. McKee M, Stuckler D (2020) If the world fails to protect the economy, COVID-19 will damage health not just now but also in the future. Nat Med 26:640–642
4. Sanders JM, Monogue ML, Jodlowski TZ, Cutrell JB (2020) Pharmacologic treatments for coronavirus disease 2019 (COVID-19): a review. JAMA - J Am Med Assoc 323:1824–1836
5. Kevadiya BD, Machhi J, Herskovitz J et al (2021) Diagnostics for SARS-CoV-2 infections. Nat Mater 20:593–605
6. CDC: COVID-19 Dashoard. https://www.cdc.gov/coronavirus/2019-ncov/hcp/duration-isolation.html. Accessed 18 Oct 2021
7. Udugama B, Kadhiresan P, Kozlowski HN et al (2020) Diagnosing COVID-19: the disease and tools for detection. ACS Nano 14:3822–3835
8. Freeman WM, Walker SJ, Kent VE (1975) Quantitative RT-PCR: pitfalls and potential. Arzneimittel-Forschung/Drug Res 25:1460–1463
9. Xiao SY, Wu Y, Liu H (2020) Evolving status of the 2019 novel coronavirus infection: Proposal of conventional serologic assays for disease diagnosis and infection monitoring. J Med Virol 92:464–467
10. Bernheim A, Mei X, Huang M et al (2020) Chest CT findings of coronavirus disease 2019 (COVID-19): relationship to duration of infection. Radiology 30:200463
11. Lamb LE, Bartolone SN, Ward E, Chancellor MB (2020) Rapid detection of novel coronavirus/Severe Acute Respiratory Syndrome Coronavirus 2 (SARS-CoV-2) by reverse transcription-loop-mediated isothermal amplification. PLoS ONE 15: e0234682
12. Kellner MJ, Koob JG, Gootenberg JS et al (2019) SHERLOCK: nucleic acid detection with CRISPR nucleases. Nat Protoc 14:2986–3012
13. Zhang W, Du RH, Li B et al (2020) Molecular and serological investigation of 2019-nCoV infected patients: implication of multiple shedding routes. Emerg Microbes Infect 9:386–389
14. Moitra P, Alafeef M, Alafeef M et al (2020) Selective naked-eye detection of SARS-CoV-2 mediated by N gene targeted antisense oligonucleotide capped plasmonic nanoparticles. ACS Nano 14:7617–7627
15. Seo G, Lee G, Kim MJ et al (2020) Rapid detection of COVID-19 causative virus (SARS-CoV-2) in human nasopharyngeal swab specimens using field-effect transistor-based biosensor. ACS Nano 14:5135–5142
16. della Ventura B, Cennamo M, Minopoli A et al (2020) Colorimetric test for fast detection of SARS-CoV-2 in nasal and throat swabs. ACS Sens 5:3043–3048
17. Niikura K, Nagakawa K, Ohtake N et al (2009) Gold nanoparticle arrangement on viral particles through carbohydrate recognition:

a non-cross-linking approach to optical virus detection. Bioconjugate Chem 20:1848–1852
18. Zheng L, Wei J, Lv X et al (2017) Detection and differentiation of influenza viruses with glycan-functionalized gold nanoparticles. Biosens Bioelectron 91:46–52
19. Vlachakis D, Papakonstantinou E, Mitsis T, Pierouli K, Diakou I, Chrousos G, Bacopoulou F (2020) Molecular mechanisms of the novel coronavirus SARS-CoV-2 and potential anti-COVID19 pharmacological targets since the outbreak of the pandemic. Food Chem Toxicol 146:111805
20. Tai W, He L, Zhang X et al (2020) Characterization of the receptor-binding domain (RBD) of 2019 novel coronavirus: implication for development of RBD protein as a viral attachment inhibitor and vaccine. Cell Mol Immunol 17:613–620
21. Lan J, Ge J, Yu J et al (2020) Structure of the SARS-CoV-2 spike receptor-binding domain bound to the ACE2 receptor. Nature 581:215–220
22. Lim Y, Ng Y, Tam J, Liu D (2016) Human coronaviruses: a review of virus–host interactions. Diseases 4:26
23. Medhi R, Srinoi P, Ngo N et al (2020) Nanoparticle-based strategies to combat COVID-19. ACS Appl Nano Mater 3:8557–8580
24. Pramanik A, Gao Y, Patibandla S et al (2021) The rapid diagnosis and effective inhibition of coronavirus using spike antibody attached gold nanoparticles. Nanoscale Adv 3:1588–1596
25. Liu Y, Zhang L, Wei W et al (2015) Colorimetric detection of influenza A virus using antibody-functionalized gold nanoparticles. Analyst 140:3989–3995
26. Badhe Y, Gupta R, Rai B (2021) In silico design of peptides with binding to the receptor binding domain (RBD) of the SARS-CoV-2 and their utility in bio-sensor development for SARS-CoV-2 detection. RSC Adv 11:3816–3826
27. Woo H, Park SJ, Choi YK et al (2020) Developing a fully glycosylated full-length SARS-COV-2 spike protein model in a viral membrane. J Phys Chem B 124:7128–7137
28. Choi YK, Cao Y, Frank M et al (2021) Structure, dynamics, receptor binding, and antibody binding of the fully glycosylated full-length SARS-CoV-2 spike protein in a viral membrane. J Chem Theory Comput 17:2479–2487
29. Monticelli L, Kandasamy SK, Periole X et al (2008) The MARTINI coarse-grained force field: extension to proteins. J Chem Theory Comput 4:819–834
30. martinize. http://cgmartini.nl/index.php/tools2/proteins-and-bilayers/204-martinize. Accessed 11 Apr 2022
31. Wassenaar TA, Pluhackova K, Böckmann RA, Marrink SJ, Tieleman DP (2014) Going backward: a flexible geometric approach to reverse transformation from coarse grained to atomistic models. J Chem Theory Comput 10:676–690
32. Lin J, Zhang H, Chen Z, Zheng Y (2010) Penetration of lipid membranes by gold nanoparticles: insights into cellular uptake, cytotoxicity, and their relationship. ACS Nano 4:5421–5429
33. Lin JQ, Zhang HW, Chen Z et al (2011) Simulation study of aggregations of monolayer-protected gold nanoparticles in solvents. J Phys Chem C 115:18991–18998
34. Gupta R, Rai B (2017) Effect of size and surface charge of gold nanoparticles on their skin permeability: a molecular dynamics study. Sci Rep 7:1–13
35. Zarabi MF, Arshadi N, Farhangi A, Akbarzadeh A (2014) Preparation and characterization of gold nanoparticles with amino acids, examination of their stability. Indian J Clin Biochem 29:306–314. https://doi.org/10.1007/s12291-013-0358-4
36. Abraham MJ, Murtola T, Schulz R et al (2015) Gromacs: High performance molecular simulations through multi-level parallelism from laptops to supercomputers. SoftwareX 1–2:19–25
37. Hess B, Kutzner C, Van Der Spoel D, Lindahl E (2008) GROMACS 4: algorithms for highly efficient, load-balanced, and scalable molecular simulation. J Chem Theory Comput 4:435–447
38. Pronk S, Páll S, Schulz R et al (2013) GROMACS 4.5: A high-throughput and highly parallel open source molecular simulation toolkit. Bioinformatics 29:845–854
39. Humphrey W, Dalke A, Schulten K (1996) VMD: visual molecular dynamics. J Mol Graph 14:33–38
40. Kumar S, Rosenberg JM, Bouzida D et al (1992) THE weighted histogram analysis method for free-energy calculations on biomolecules. I. The method. J Comput Chem 13:1011–1021
41. Liu S, Lämmerhofer M (2019) Functionalized gold nanoparticles for sample preparation: a review. Electrophoresis 40:2438–2461
42. Froloff N, Windemuth A, Honig B (1997) On the calculation of binding free energies using continuum methods: application to MHC class I protein-peptide interactions. Protein Sci 6:1293–1301
43. Wang J, Alekseenko A, Kozakov D, Miao Y (2019) Improved modeling of peptide-protein binding through global docking and accelerated molecular dynamics simulations. Front Mol Biosci 6:1–10
44. de Jong DH, Singh G, Bennett WFD et al (2013) Improved parameters for the martini coarse-grained protein force field. J Chem Theory Comput 9:687–697
45. Bachmann MF, Mohsen MO, Zha L, Vogel M, Speiser DE (2021) SARS-CoV-2 structural features may explain limited neutralizing-antibody responses. npj Vaccines 6:2